Formation of multiscale surface structures on nickel via above surface growth and below surface growth mechanisms using femtosecond laser pulses

Craig A. Zuhlke,* Troy P. Anderson, and Dennis R. Alexander

Department of Electrical Engineering, University of Nebraska – Lincoln, 209N Scott Engineering Center, Lincoln, NE 68588, USA

**czuhlke11@gmail.com*

Abstract: The formation of self-organized micro- and nano-structured surfaces on nickel via both above surface growth (ASG) and below surface growth (BSG) mechanisms using femtosecond laser pulse illumination is reported. Detailed stepped growth experiments demonstrate that conical mound-shaped surface structure development is characterized by a balance of growth mechanisms including scattering from surface structures and geometric effects causing preferential ablation of the valleys, flow of the surface melt, and redeposition of ablated material; all of which are influenced by the laser fluence and the number of laser shots on the sample. BSG-mound formation is dominated by scattering, while ASG-mound formation is dominated by material flow and redeposition. This is the first demonstration to our knowledge of the use of femtosecond laser pulses to fabricate metallic surface structures that rise above the original surface. These results are useful in understanding the details of multi-pulse femtosecond laser interaction with metals.

OCIS codes: (320.2250) Femtosecond phenomena; (140.3390) Laser materials processing; (240.5770) Roughness.

References and links

1. B. G. Lee, H. M. Branz, Y.-T. Lin, E. Mazur, and M.-J. Sher, "Light trapping for thin silicon solar cells by femtosecond laser texturing preprint," in IEEE Phot. Spec. Conf (2012).
2. H. Wang, P. Kongsuwan, G. Satoh, and Y. Lawrence Yao, "Femtosecond laser-induced simultaneous surface texturing and crystallization of a-Si:H thin film: absorption and crystallinity," J. Manuf. Sci. Eng. 134(3), 031006 (2012).
3. H. Wang, P. Kongsuwan, G. Satoh, and Y. L. Yao, "Effect of processing medium and condition on absorption enhancement of femtosecond laser treated a-Si: H thin film," Proceedings of NAMRI 39, (2011).
4. M.-J. Sher, M. T. Winkler, and E. Mazur, "Pulsed-laser hyperdoping and surface texturing for photovoltaics," MRS Bull. 36(06), 439–445 (2011).
5. V. V. Iyengar, B. K. Nayak, and M. C. Gupta, "Optical properties of silicon light trapping structures for photovoltaics," Sol. Energy Mater. Sol. Cells 94(12), 2251–2257 (2010).
6. M. Halbwax, T. Sarnet, P. Delaporte, M. Sentis, H. Etienne, F. Torregrosa, V. Vervisch, I. Perichaud, and S. Martinuzzi, "Micro and nano-structuration of silicon by femtosecond laser: Application to silicon photovoltaic cells fabrication," Thin Solid Films 516(20), 6791–6795 (2008).
7. A. Serpengüzel, A. Kurt, I. Inanç, J. Cary, E. Mazur, A. Serpenguzel, I. Inanç, and J. E. Carey III, "Luminescence of black silicon," J. Nanophotonics 2(1), 021770 (2008).
8. B. K. Nayak and M. C. Gupta, "Femtosecond-laser-induced-crystallization and simultaneous formation of light trapping microstructures in thin a-Si:H films," Appl. Phys. Adv. Mater. 89, 663–666 (2007).
9. J. E. Carey, C. H. Crouch, and E. Mazur, "Femtosecond-laser-assisted microstructuring of silicon surfaces," Lasers and Electro-Optics Society (LEOS) (2003), pp. 97–98.
10. R. Younkin, J. E. Carey III, E. Mazur, J. A. Levinson, and C. M. Friend, "Infrared absorption by conical silicon microstructures made in a variety of background gases using femtosecond-laser pulses," Jpn. J. Appl. Phys. 93(5), 2626 (2003).

#185267 - $15.00 USD Received 13 Feb 2013; revised 22 Mar 2013; accepted 22 Mar 2013; published 29 Mar 2013

11. A. Y. Vorobyev and C. Guo, "Laser turns silicon superwicking," Opt. Express 18(7), 6455–6460 (2010).
12. A. Y. Vorobyev and C. Guo, "Water sprints uphill on glass," Jpn. J. Appl. Phys. 108(12), 123512 (2010).
13. B. Wu, M. Zhou, J. Li, X. Ye, G. Li, and L. Cai, "Superhydrophobic surfaces fabricated by microstructuring of stainless steel using a femtosecond laser," Appl. Surf. Sci. 256(1), 61–66 (2009).
14. A.-M. Kietzig, S. G. Hatzikiriakos, and P. Englezos, "Patterned superhydrophobic metallic surfaces," Langmuir 25(8), 4821–4827 (2009).
15. E. Fadeeva, V. K. Truong, M. Stiesch, B. N. Chichkov, R. J. Crawford, J. Wang, and E. P. Ivanova, "Bacterial retention on superhydrophobic titanium surfaces fabricated by femtosecond laser ablation," Langmuir 27(6), 3012–3019 (2011).
16. P. Bizi-Bandoki, S. Benayoun, S. Valette, B. Beaugiraud, and E. Audouard, "Modifications of roughness and wettability properties of metals induced by femtosecond laser treatment," Appl. Surf. Sci. 257(12), 5213–5218 (2011).
17. B. K. Nayak, M. C. Gupta, and K. W. Kolasinski, "Spontaneous formation of nanospiked microstructures in germanium by femtosecond laser irradiation," Nanotechnology 18(19), 195302 (2007).
18. J. Bonse, S. Baudach, J. Krüger, W. Kautek, and M. Lenzner, "Femtosecond laser ablation of silicon-modification thresholds and morphology," Appl. Phys. Adv. Mater. 74, 19–25 (2002).
19. K. W. Kolasinski, D. Mills, and M. Nahidi, "Laser assisted and wet chemical etching of silicon nanostructures," J. Vac. Sci. Technol. A 24(4), 1474 (2006).
20. V. Zorba, N. Boukos, I. Zergioti, and C. Fotakis, "Ultraviolet femtosecond, picosecond and nanosecond laser microstructuring of silicon: structural and optical properties," Appl. Opt. 47(11), 1846–1850 (2008).
21. J. Zhu, G. Yin, M. Zhao, D. Chen, and L. Zhao, "Evolution of silicon surface microstructures by picosecond and femtosecond laser irradiations," Appl. Surf. Sci. 245(1-4), 102–108 (2005).
22. V. Zorba, I. Alexandrou, I. Zergioti, A. Manousaki, C. Ducati, A. Neumeister, C. Fotakis, and G. A. J. Amaratunga, "Laser microstructuring of Si surfaces for low-threshold field-electron emission," Thin Solid Films 453–454, 492–495 (2004).
23. T. Yong Hwang and C. Guo, "Polarization and angular effects of femtosecond laser-induced conical microstructures on Ni," Jpn. J. Appl. Phys. 111(8), 083518 (2012).
24. T. H. Her, R. J. Finlay, C. Wu, and E. Mazur, "Femtosecond laser-induced formation of spikes on silicon," Appl. Phys. Adv. Mater. 70, 383–385 (2000).
25. B. R. Tull, J. E. Carey III, E. Mazur, J. P. McDonald, and S. M. Yalisove, "Silicon surface morphologies after femtosecond laser irradiation," MRS Bull. 31(08), 626–633 (2006).
26. C. H. Crouch, J. E. Carey III, J. M. Warrender, M. J. Aziz, E. Mazur, and F. Y. Génin, "Comparison of structure and properties of femtosecond and nanosecond laser-structured silicon," Appl. Phys. Lett. 84(11), 1850 (2004).
27. T.-H. Her, R. J. Finlay, C. Wu, S. Deliwala, and E. Mazur, "Microstructuring of silicon with femtosecond laser pulses," Appl. Phys. Lett. 73(12), 1673 (1998).
28. B. K. Nayak, M. C. Gupta, and K. W. Kolasinski, "Ultrafast-laser-assisted chemical restructuring of silicon and germanium surfaces," Appl. Surf. Sci. 253(15), 6580–6583 (2007).
29. M. A. Sheehy, L. Winston, J. E. Carey, C. M. Friend, and E. Mazur, "Role of the background gas in the morphology and optical properties of laser-microstructured silicon," Chem. Mater. 17(14), 3582–3586 (2005).
30. D. Riedel, J. L. Hernandez-Pozos, R. E. Palmer, and K. W. Kolasinski, "Fabrication of ordered arrays of silicon cones by optical diffraction in ultrafast laser etching with SF6," Appl. Phys. Adv. Mater. 78, 381–385 (2004).
31. B. K. Nayak and M. C. Gupta, "Ultrafast laser-induced self-organized conical micro/nano surface structures and their origin," Opt. Lasers Eng. 48(10), 966–973 (2010).
32. K. Kuršelis, R. Kiyan, and B. N. Chichkov, "Formation of corrugated and porous steel surfaces by femtosecond laser irradiation," Appl. Surf. Sci. 258(22), 8845–8852 (2012).
33. V. Dumas, A. Rattner, L. Vico, E. Audouard, J. C. Dumas, P. Naisson, and P. Bertrand, "Multiscale grooved titanium processed with femtosecond laser influences mesenchymal stem cell morphology, adhesion, and matrix organization," J. Biomed. Mater. Res. A 100(11), 3108–3116 (2012).
34. B. K. Nayak and M. C. Gupta, "Self-organized micro/nano structures in metal surfaces by ultrafast laser irradiation," Opt. Lasers Eng. 48(10), 940–949 (2010).
35. Y. Yang, J. Yang, C. Liang, H. Wang, X. Zhu, and N. Zhang, "Surface microstructuring of Ti plates by femtosecond lasers in liquid ambiences: a new approach to improving biocompatibility," Opt. Express 17(23), 21124–21133 (2009).
36. C. Liang, Y. Yang, H. Wang, J. Yang, and X. Yang, "Preparation of porous microstructures on NiTi alloy surface with femtosecond laser pulses," Chin. Sci. Bull. 53(5), 700–705 (2008).
37. N. G. Semaltianos, W. Perrie, P. French, M. Sharp, G. Dearden, and K. G. Watkins, "Femtosecond laser surface texturing of a nickel-based superalloy," Appl. Surf. Sci. 255(5), 2796–2802 (2008).
38. N. G. Semaltianos, W. Perrie, P. French, M. Sharp, G. Dearden, S. Logothetidis, and K. G. Watkins, "Femtosecond laser ablation characteristics of nickel-based superalloy C263," Appl. Phys. Adv. Mater. 94, 999–1009 (2008).
39. A. Y. Vorobyev and C. Guo, "Femtosecond laser structuring of titanium implants," Appl. Surf. Sci. 253(17), 7272–7280 (2007).
40. M. Tsukamoto, T. Kayahara, H. Nakano, M. Hashida, M. Katto, M. Fujita, M. Tanaka, and N. Abe, "Microstructures formation on titanium plate by femtosecond laser ablation," J. Phys. Conf. Ser. 59, 666–669 (2007).

#185267 - $15.00 USD Received 13 Feb 2013; revised 22 Mar 2013; accepted 22 Mar 2013; published 29 Mar 2013

41. W. Jia, Z. Peng, Z. Wang, X. Ni, and C. Wang, "The effect of femtosecond laser micromachining on the surface characteristics and subsurface microstructure of amorphous FeCuNbSiB alloy," Appl. Surf. Sci. 253(3), 1299–1303 (2006).
42. P. T. Mannion, J. Magee, E. Coyne, G. M. O'Connor, and T. J. Glynn, "The effect of damage accumulation behaviour on ablation thresholds and damage morphology in ultrafast laser micro-machining of common metals in air," Appl. Surf. Sci. 233(1-4), 275–287 (2004).
43. M. Bereznai, I. Pelsöczi, Z. Tóth, K. Turzó, M. Radnai, Z. Bor, and A. Fazekas, "Surface modifications induced by ns and sub-ps excimer laser pulses on titanium implant material," Biomaterials 24(23), 4197–4203 (2003).
44. G. Dumitru, V. Romano, H. P. Weber, M. Sentis, and W. Marine, "Femtosecond ablation of ultrahard materials," Appl. Phys. Adv. Mater. 74, 729–739 (2002).
45. B. K. Nayak, M. C. Gupta, and K. W. Kolasinski, "Formation of nano-textured conical microstructures in titanium metal surface by femtosecond laser irradiation," Appl. Phys. Adv. Mater. 90, 399–402 (2007).
46. A. Y. Vorobyev and C. Guo, "Direct femtosecond laser surface nano/microstructuring and its applications," Laser Photonics Rev. 1 – 23 (2012).
47. B. K. Nayak and M. C. Gupta, "Self-organized micro/nano structures in metal surfaces by ultrafast laser irradiation," Opt. Lasers Eng. 48(10), 940–949 (2010).
48. V. V. Iyengar, B. K. Nayak, and M. C. Gupta, "Ultralow reflectance metal surfaces by ultrafast laser texturing," Appl. Opt. 49(31), 5983 (2010).
49. A. Y. Vorobyev and C. Guo, "Enhanced absorptance of gold following multipulse femtosecond laser ablation," Phys. Rev. B 72(19), 195422 (2005).
50. G. D. Tsibidis, M. Barberoglou, P. A. Loukakos, E. Stratakis, and C. Fotakis, "Dynamics of ripple formation on silicon surfaces by ultrashort laser pulses in subablation conditions," Phys. Rev. B 86(11), 115316 (2012).
51. M. Y. Shen, C. H. Crouch, J. E. Carey III, R. Younkin, E. Mazur, M. Sheehy, and C. M. Friend, "Formation of regular arrays of silicon microspikes by femtosecond laser irradiation through a mask," Appl. Phys. Lett. 82(11), 1715 (2003).
52. A. P. Singh, A. Kapoor, K. N. Tripathi, and G. R. Kumar, "Laser damage studies of silicon surfaces using ultra-short laser pulses," Opt. Laser Technol. 34(1), 37–43 (2002).
53. F. Sánchez, J. L. Morenza, R. Aguiar, J. C. Delgado, and M. Varela, "Dynamics of the hydrodynamical growth of columns on silicon exposed to ArF excimer-laser irradiation," Appl. Phys. Adv. Mater. 66, 83–86 (1998).
54. F. Sanchez, J. L. Morenza, and V. Trtik, "Characterization of the progressive growth of columns by excimer laser irradiation of silicon," Appl. Phys. Lett. 75(21), 3303 (1999).
55. S. I. Dolgaev, S. V. Lavrishev, A. A. Lyalin, A. V. Simakin, V. V. Voronov, and G. A. Shafeev, "Formation of conical microstructures upon laser evaporation of solids," Appl. Phys. Adv. Mater. 73, 177–181 (2001).
56. D. H. Lowndes, J. D. Fowlkes, and A. J. Pedraza, "Early stages of pulsed-laser growth of silicon microcolumns and microcones in air and SF6," Appl. Surf. Sci. 154–155, 647–658 (2000).
57. D. Mills and K. W. Kolasinski, "Solidification driven extrusion of spikes during laser melting of silicon pillars," Nanotechnology 17(11), 2741–2744 (2006).
58. A. J. Pedraza, J. D. Fowlkes, S. Jesse, C. Mao, and D. H. Lowndes, "Surface micro-structuring of silicon by excimer-laser irradiation in reactive atmospheres," Appl. Surf. Sci. 168(1-4), 251–257 (2000).
59. A. J. Pedraza, J. D. Fowlkes, and D. H. Lowndes, "Self-organized silicon microcolumn arrays generated by pulsed laser irradiation," Mater. Sci. 734, 731–734 (2008).
60. A. J. Pedraza, J. D. Fowlkes, and D. H. Lowndes, "Silicon microcolumn arrays grown by nanosecond pulsed-excimer laser irradiation," Appl. Phys. Lett. 74(16), 2322–2324 (1999).
61. A. J. Pedraza, J. D. Fowlkes, and D. H. Lowndes, "Laser ablation and column formation in silicon under oxygen-rich atmospheres," Appl. Phys. Lett. 77(19), 3018 (2000).
62. F. Sanchez, J. L. Morenza, R. Aguiar, J. C. Delgado, and M. Varela, "Whiskerlike structure growth on silicon exposed to ArF excimer laser irradiation," Appl. Phys. Lett. 69(5), 620 (1996).
63. V. V. Voronov, S. I. Dolgaev, S. V. Lavrishchev, A. A. Lyalin, A. V. Simakin, and G. A. Shafeev, "Formation of conic microstructures upon pulsed laser evaporation of solids," Quantum Electron. 30(8), 710–714 (2000).
64. R. S. Wagner and W. C. Ellis, "Vapor-liquid-solid mechanism of single crystal growth," Appl. Phys. Lett. 4(5), 89 (1964).
65. J. Bonse, J. Krüger, S. Höhm, and A. Rosenfeld, "Femtosecond laser-induced periodic surface structures," J. Laser Appl. 24(4), 042006 (2012).
66. H. van Driel, J. Sipe, and J. Young, "Laser-Induced Periodic Surface Structure on Solids: A Universal Phenomenon," Phys. Rev. Lett. 49(26), 1955–1958 (1982).
67. J. E. Sipe, J. F. Young, J. S. Preston, and H. M. van Driel, "Laser-induced periodic surface structure. I. Theory," Phys. Rev. B 27(2), 1141–1154 (1983).

Introduction

Functionalized surfaces with tailored optical, electrical, chemical, and wettability properties can be fabricated using femtosecond laser surface structuring; engineered surface properties are obtained by the production of self-organized micro- and nano-scale features. Functionalized surfaces are critical for a broad range of commercial and industrial

#185267 - $15.00 USD Received 13 Feb 2013; revised 22 Mar 2013; accepted 22 Mar 2013; published 29 Mar 2013

applications. Perhaps the most well-known application of such a functionalized surface is the production of black silicon, which exhibits wide-band optical absorption for increased solar cell efficiency [1–10]. Additionally, the modification of wettability from superhydrophilic [11,12] to superhydrophobic [13–16] is utilized for self-cleaning surfaces, drag reduction, and anticorrosive surfaces, among others.

To date, most of the work using lasers for surface texturing has focused on what have been called pillars [5,17–19], cones [20–23] or spikes [18,24–26]. These are generally tightly-packed self-organized structures with an aspect ratio of 2:1 or higher that develop over a series of tens to hundreds of laser shots. The structures take the shape of either a cylinder, sharp cone, or rounded cone, have dimensions of up to tens of microns in both height and diameter, and are typically covered in a layer of nanoparticles. The physical mechanisms attributed to the formation of these multi-scale surface structures are highly dependent on the properties of the substrate material as well as on the specific illumination conditions including the laser fluence, repetition rate, number of pulses incident on the sample, and the atmospheric conditions during processing.

A comprehensive model has yet to be developed that can accurately describe the formation of multi-scale surface structures via multi-pulse femtosecond laser irradiation over a wide range of conditions due to the complex light-matter interaction and the high number of processing parameters involved. Instead, most published descriptions of laser functionalized surfaces detail a specific structure geometry and relevant applications. A detailed description of the formation and growth of micro/nanostructures using femtosecond laser pulses in multiple atmospheric environments including SF_6 has been published for silicon [3,10,24,25,27–31], including the well-known "black silicon" [4,24–26]. In addition to silicon, the formation of micro/nanostructures using femtosecond pulses has been studied on a number of metals [13,16,32–44], and in different atmospheres [45]. However, although multiple structure types ranging from LIPSS to complex multi-scale features have been fabricated on metals [14,23,32,38–40,46,47], a detailed understanding of the effect of laser processing parameters (e.g. fluence and the number of shots) on the balance of different growth mechanisms is still lacking.

In the current paper, we provide a detailed scanning electron microscope (SEM) shot-by-shot analysis of the development of two distinct multi-scale surface formation processes on nickel, which will be referred to as *BSG-mounds* (below surface growth mounds) and *ASG-mounds* (above surface growth mounds). BSG-mounds always have peaks below the original surface and are representative of the most frequently published self-organized microstructures that form on metals via focused femtosecond laser illumination [14,23,32,34,38–40,48]. In contrast, ASG-mounds exhibit upward growth and result in structures with peaks above the original surface. A series of shot-by-shot SEM images of the same area provides insight into the dominant growth mechanisms of each structure type. The formation of BSG-mounds is dominated by preferential valley ablation (PVA), whereas the formation of ASG-mounds is dominated by fluid flow and redeposition of ablated material. Although structures growing above the original surface have been demonstrated with femtosecond pulse ablation of silicon [18], this is the first demonstration to our knowledge of metallic surface structures fabricated by femtosecond laser pulse illumination that grow above the original surface. This study provides a significant advancement toward a broader understanding of the formation of multi-scale surface structures in metals that may ultimately lead to precise tailoring of surfaces for specific applications.

Experiment

The growth mechanisms of self-organized surface structures on metallic surfaces were studied by alternately illuminating the sample with one (or more) femtosecond laser pulses and then subsequently imaging the processed surface using a Philips XL-30 Environmental Scanning Electron Microscope (SEM) manufactured by FEI Company. After each SEM

#185267 - $15.00 USD Received 13 Feb 2013; revised 22 Mar 2013; accepted 22 Mar 2013; published 29 Mar 2013

image was taken, the sample was precisely realigned to the same location in the laser setup using mechanical guides and high optical magnification imaging (located above the illumination area). The shot-by-shot growth of surface structures is thus captured using a series of SEM images that can be analyzed individually or sequenced as frames and viewed as a stop-motion video. Each time the sample was imaged in the SEM, images were saved at a number of locations, magnifications, and viewing angles. This process was carried out for two values of laser fluence: 1.39 J/cm^2 and 3.08 J/cm^2. These fluence values were chosen by studying a series of ablation craters produced using a range of fluence values and pulse counts. With increasing fluence, there appears to be a transition from BSG-mound formation to ASG-mound formation around 2 J/cm^2. Therefore, 1.39 J/cm^2 and 3.08 J/cm^2 were chosen to ensure the structures that form at each fluence would be unique. A detailed study of surface structure formation over a wide fluence range will be described in a later publication. The number of pulses between SEM imaging was varied for each fluence value to balance the time commitment and the step size over which interesting results could be observed. Through the use of this stop-motion SEM technique, subtle variations in the dominant growth mechanisms could be observed for the first time and reported as a function of laser fluence.

The laser used for carrying out this research was a Spectra Physics Spitfire, Ti:Sapphire femtosecond laser system. The system is capable of producing 1 mJ, 50 fs pulses. In combination with a computer-controlled shutter, the repetition rate of the laser is adjustable from single pulses up to the maximum of 1 kHz. The pulse length and chirp were monitored using a Frequency Resolved Optical Gating (FROG) instrument from Positive Light (Model 8-02). The position of the sample with respect to the laser focal volume was controlled using computer-guided Melles Griot nanomotion translation stages with 3 axes of motion. The laser power was controlled using a half waveplate and a polarizer.

Previous studies have demonstrated that the growth of self-organized surface structures is critically dependent on the laser fluence. For this reason, a square-shaped flat-top beam profile with 150 μm sides (see Fig. 1) was used for the experiments in order to generate a uniform laser fluence on the material surface. This beam profile was created using a refractive beam shaper from Eksma Optics (GTH-4-2.2FA). The laser fluence varied by less than 20% across the central portion of the beam. Fluence fluctuations in the flat-top distribution are attributed to the asymmetries and inhomogeneity of the input beam. The flat-top profile does not change within the 50 μm ablation depths studied in this work. The spot size on the sample was determined by taking the average side length (the absolute edge of ablation seen in the SEM) of 10 sets of 100 pulse ablation spots with the laser power adjusted to produce 1.4 J/cm^2 on the surface. With more than 100 pulses, in a single spot, redeposition of nanoparticles around the outer edges of the ablation spot cause it to appear smaller than the actual spot size and with less than 100 pulses, the ablation spot appears smaller because the ablation on the very edges of the spot, where the fluence quickly drops off, cannot be seen in the SEM. Figure 1 is a diagram of the experimental setup. The work presented here was completed using nickel, which was chosen because of its promising use as electrodes in pseudocapacitor and electrolysis systems, its purity, and the amount of published work on femtosecond pulse interactions with nickel.

#185267 - $15.00 USD Received 13 Feb 2013; revised 22 Mar 2013; accepted 22 Mar 2013; published 29 Mar 2013

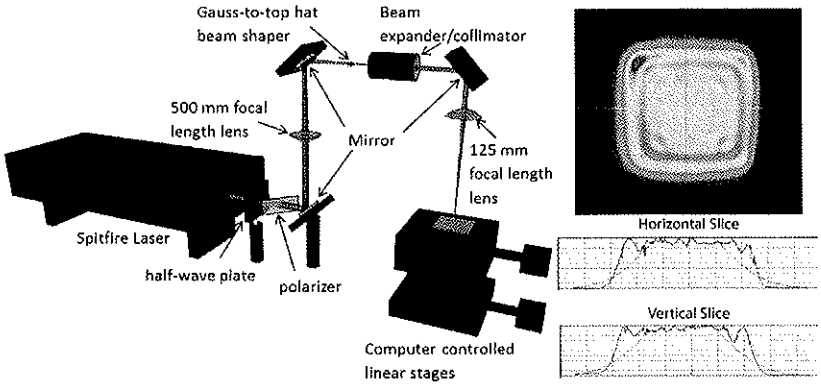

Fig. 1. (left) Experimental setup utilized in this paper. (right) Flat-top beam profile as measured by beam profiler.

Results and discussion

The growth of multi-scale surface features via femtosecond laser illumination can be broadly characterized by three phases. The first phase is the introduction of roughness on the nanometer and micrometer scales that ultimately leads to the creation of precursor sites that affect the distribution of laser energy from subsequent laser pulses on the sample. The second phase of growth is the development of the precursor sites to form larger self-organized features. The third phase represents the evolution of the self-organized structures upon continued illumination. The laser fluence has a significant impact on both the development of the precursor sites as well as the dominant growth mechanism after the precursor sites are established. Surface structures fabricated with laser fluence values of 1.39 J/cm^2 and 3.08 J/cm^2 are seen to differ greatly in both the observed formation mechanisms and the final morphology. Specifically, surface structures formed with a laser fluence of 1.39 J/cm^2 are characterized by features that lie at or below the original surface and are referred to as below-surface-growth (BSG)-mounds. In contrast, surface structures formed with a laser fluence of 3.08 J/cm^2 are characterized by features that rise above the original surface as well as by the presence of large ablation pits that dominate the surface for pulse counts higher than 200. These structures are referred to as above-surface-growth (ASG)-mounds. The following paragraphs detail the formation of both structure types.

First phase: generation of precursor sites

The initial stage of formation is qualitatively similar for both BSG-mounds and ASG-mounds, with the primary difference being the number of laser pulses involved. At low pulse counts (up to ~15 pulses for ASG-mounds and ~50 pulses for BSG-mounds), the surface is covered with random nanostructures. With each shot, the random nanostructure is destroyed and new random nanostructure is created; the geometric surface pattern is not preserved between successive shots. This can be seen in the images taken from successive SEM images in Fig. 2(a)–2(d). With increasing laser shot count, the nanostructure becomes larger and denser. The shift towards larger and denser structures is attributed to increased absorption by nanoparticles on the surface produced from previous pulses as well as geometric effects caused by scattering from the increasingly roughened surface. This random nanostructure develops through hydrodynamical processes, such as fluid flow of the surface melt due to surface tension gradients, as well as through the formation of nanocavities due to cavitation bubbles [39,46,49,50]. For a given number of laser pulses on the sample, the nanostructure is

#185267 - $15.00 USD Received 13 Feb 2013; revised 22 Mar 2013; accepted 22 Mar 2013; published 29 Mar 2013

larger using 3.08 J/cm^2 than using 1.39 J/cm^2 as illustrated in Fig. 2(e) and 2(f). Furthermore, the development of micron-sized surface structures through this process occurs with fewer pulses for the larger laser fluence.

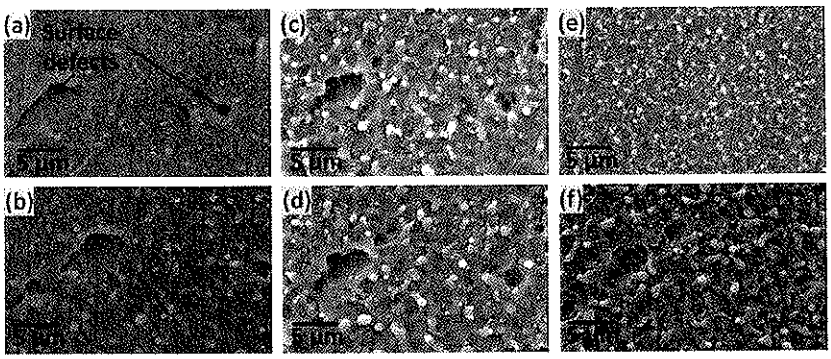

Fig. 2. (a) – (d) SEM images of the same location on nickel (200/201) ablated at 3.08 J/cm^2 with (a) 1, (b) 2, (c) 5 and (d) 6 pulses. (e) and (f) SEM images of different nickel samples ablated with 10 pulses at (e) 1.39 J/cm^2 and (f) 3.08 J/cm^2.

Continued illumination of the random nanostructure with femtosecond laser pulses results in the evolution of micron-scale self-organized features, referred to here as precursor sites. The precursor site formation takes place in two ways. The first is with the formation of micro-ripples (periodic ripples that form parallel to the incident pulse polarization with a period that is fluence dependent ranging from 2.5 – 5 μm [16,32,38–41,51,52]). Along the peaks of these micro-ripples, domes form with a diameter similar to the micro-ripple size (see Fig. 3). These structures are the only form of precursor site observed for the formation of BSG-mounds in this work. With ASG-mound development, a second formation process for precursor sites occurs in some cases. In this case, the first microstructure formation observed is pitting of the surface. With increased pulse count, the pits grow deeper and rims form from displaced material. Along these rims, domes form that then act as the precursor sites. This process can be seen in Fig. 4, where the formation of a pit can be seen at the location marked 1, followed by the formation of a dome (marked 2) along the rim around the pit. In this example, the pit formation started at a defect present in the sample before processing, but in some cases the pits form at locations where surface defects are not visible using a SEM for imaging.

#185267 - $15.00 USD Received 13 Feb 2013; revised 22 Mar 2013; accepted 22 Mar 2013; published 29 Mar 2013

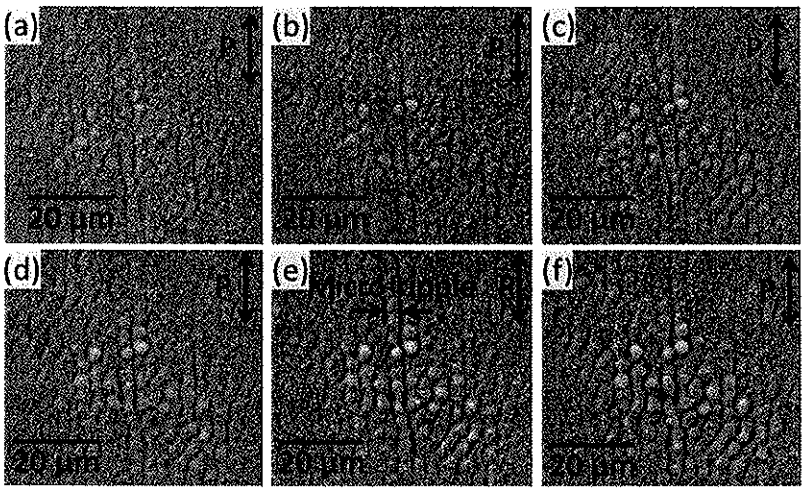

Fig. 3. SEM images of nickel (200/201) ablated with (a) 80, (b) 90, (c) 100, (d) 110, (e) 120, and (f) 130 pulses at 1.392 J/cm^2. Note the formation of micro-ripples parallel to the laser polarization and the formation of domes on top of the micro-ripples. The polarization, P, of the incident pulses is as marked in each image.

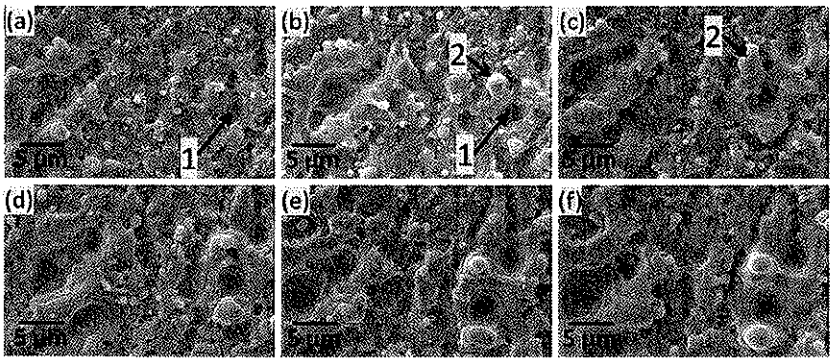

Fig. 4. SEM images of nickel (200/201) ablated with (a) 30, (b) 35, (c) 40, (d) 45, (e) 50, and (f) 55 pulses at 3.08 J/cm^2.

Second phase: development of multiscale structures and third phase: final morphology

The second phase of surface structure growth encompasses the development of multi-scale structures from the precursor sites created during the first phase. The transition between the first and second phases occurs when the presence of precursor sites significantly alters the distribution of energy of subsequent laser pulses. The laser fluence has a significant impact during this second phase on both the dominant growth mechanism and the final surface morphology. The goal of the present research is to identify which mechanisms are dominant in each of the conditions studied. Figure 5 (multimedia online) contains frames of stop-motion videos documenting the growth of the BSG-mounds (F = 1.39 J/cm^2) (see Media 1) and ASG-mounds (F = 3.08 J/cm^2) (see Media 2), respectively, viewed from a 45 degree

#185267 - $15.00 USD Received 13 Feb 2013; revised 22 Mar 2013; accepted 22 Mar 2013; published 29 Mar 2013

angle in the SEM. The top row depicts BSG-mound growth and the bottom, ASG-mound growth.

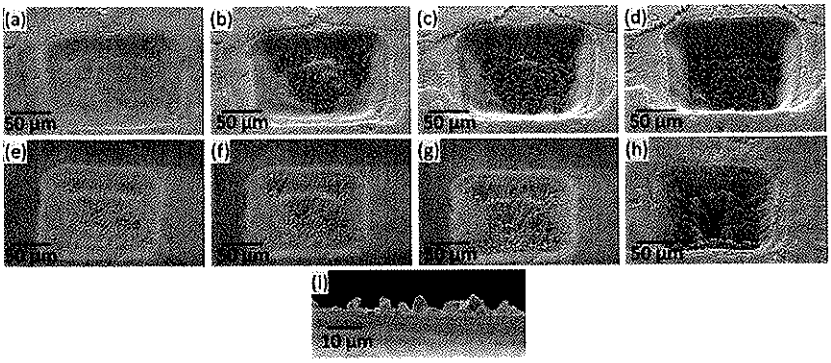

Fig. 5. (Multimedia online) Single frame excerpts of stop-motion video documenting the growth of (a) – (d) BSG-mounds (Media 1 – 1.634 Mb) and (e-h) ASG-mounds (Media 2 – 1.492 Mb) on Nickel viewed at a 45-degree angle. The number of pulses incident on the sample is 100, 300, 500, 700 for subfigures (a) – (d) and 40, 60, 80, and 300 for (e) – (h). (i) SEM image of ASG-mounds after 100 pulses viewed at a 90 degree angle demonstrating the structures that rise above the original surface.

The most direct evidence of a difference in the dominant growth mechanism for the BSG-mounds and ASG-mounds is the variations of the locations of the structure peaks and the aspect ratios of the structures. For BSG-mounds, the peaks remain below the original surface level regardless of the number of laser pulses (see Figs. 5(a)-5(d)), suggesting that the precursor sites serve to activate preferential valley ablation (PVA). PVA is a surface geometry driven process in which incoming laser light is scattered off the precursor sites generated in phase 1, resulting in increased laser fluence and a corresponding increase in ablation of the valleys between the precursor sites. The precursor sites then evolve into conical structures. Once conical structures are formed, the laser fluence on the sidewalls is decreased relative to the valleys due to increased subtended area as described by Hwang and Guo [23]. During this second phase, the conical structures grow in both height and width, while keeping the same cone angle. This growth is more readily observed in higher magnification images shown in Fig. 6 (multimedia online: Media 3). Although the ablation rates of the peaks and valleys differ, ablation is dominant and the entire irradiated area sinks below the original surface (see Media 1, Media 2, and Fig. 5(a)-5(d)). Previously published accounts on the formation of self-organized surface structures using femtosecond laser pulse illumination have been largely dominated by PVA [21,25,34,40]. The Mazur group in particular has published considerable work on the formation of conical structures on silicon processed in SF_6 using femtosecond laser pulses [4,24–26].

The third phase of BSG-mound development is characterized by the merging of the conical structures as they continue to grow, which occurs at a rapid rate after ~600 pulses under these conditions. Conical structures will merge when their growth reduces the width of the valleys and thus the effects of PVA between them. The merging process can be seen by following the BSG-mounds marked 1 and 2 in Fig. 6. Note that, once established, the BSG-mounds do not change location, but simply grow and merge with surrounding mounds, further indicating that ablation is the primary formation mechanism for these structures. Although PVA is the dominant growth mechanism, there is some indication of both fluid flow and redeposition playing a minor role. For example, the smooth sides of some mounds indicate fluid flow, but most BSG-mounds have very rough randomly textured sides more

#185267 - $15.00 USD Received 13 Feb 2013; revised 22 Mar 2013; accepted 22 Mar 2013; published 29 Mar 2013

evident of etching. Also, the hemispherical caps on the peaks of some BSG-mounds may indicate redeposition processes. However, the caps do not build on top of each other and are quickly etched away with increasing pulse count.

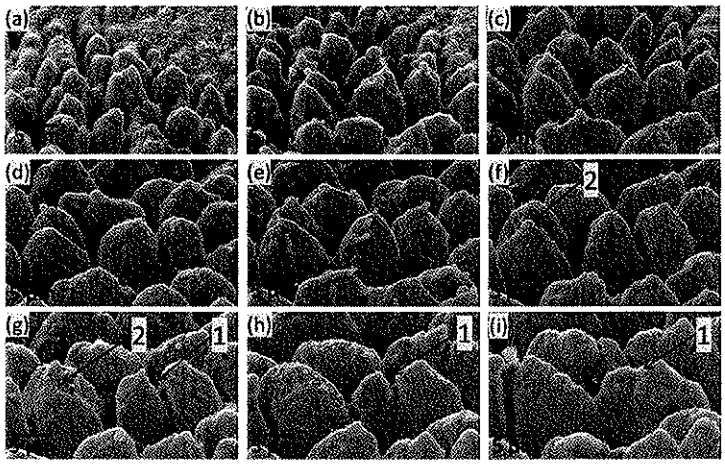

Fig. 6. (Multimedia online: Media 3 – 1.479 Mb) SEM images of stepped BSG-mound growth on nickel imaged at 45 degrees after (a) 200, (b) 300, (c) 400, (d) 500, (e) 600, (f) 700, (g) 800, (h) 900, and (i) 1000 pulses. Markers 1 and 2 point to locations where BSG-mounds combine together with increased pulse counts.

In contrast to BSG-mounds, the peaks remain near the original surface level during the second phase of ASG-mound development. As the number of pulses incident on the sample increases, PVA causes the valleys to deepen. However, a combination of fluid flow and redeposition of ablated material have a significant impact and cause the peaks to rise above the surface (see Fig. 5(i)). The fluid flow processes are likely driven by the same processes that lead to PVA. The inhomogeneous energy distribution due to the geometry of surface structures induces thermal gradients in the surface melt layer, which drives fluid flow away from the valleys between structures and up the structures themselves. This "hydrodynamical process" was attributed to the growth of columns on silicon using nanosecond pulses at laser fluence values close the ablation threshold by Sánchez et al. [53,54]. Another growth mechanism of surface structures is the redeposition of material ablated in the valleys onto the tops of the structures themselves. This mechanism has been described as vapor-liquid-solid (VLS) growth and has been used to describe the development of ASG surface structures with nanosecond pulses [26,53–64]. With VLS growth, each pulse liquefies the tops of the structures, while their steep sides lead to PVA. This results in a vapor cloud of the material around the structures, which then reacts with the melted tops, causing them to grow taller. The observation this this processes occurs during femtosecond laser structuring of metals, but only for sufficiently high fluences (it was not observed for BSG-mounds formed at F = 1.39 J/cm^2), indicates that the formation mechanisms of multiscale structures are critically dependent on fluence. A similar trend has been observed in silicon: Crouch et al. [26] observed below surface growth mechanisms for a laser fluence of 1 J/cm^2, while Bonse et al. [18] reported above growth mechanism for a fluence of 2.8 J/cm^2. The observation of this trend in both metals and semiconductors signifies the strong influence of fluence on femtosecond laser surface structuring.

Both fluid flow and material redeposition can be seen in the series of frames from the stop motion video documenting ASG-mound growth in Fig. 7 (multimedia online: Media 4). In

#185267 - $15.00 USD Received 13 Feb 2013; revised 22 Mar 2013; accepted 22 Mar 2013; published 29 Mar 2013

Fig. 7(a), a sphere on the crater wall is marked 1. With a single shot, this sphere separates into an elongated cylinder and a smaller sphere higher up the crater wall. After the next shot, the sphere has spread out and melted into the crater wall. Also notice in the transition from Fig. 7(f) and 7(g), the ASG-mound marked 2 has melted and combined with the crater wall. This transition occurs over a 5 pulse range. These structural changes demonstrate the fluid flow processes. The supplemental media files make this process more apparent. Material redeposition can also be observed in the same set of images. This process can be seen in the hemispherical caps that build up on top of the ASG-mound marked 2. With each incident pulse, a new hemispherical cap forms over the previous cap. Notice in Fig. 7(f) that several of these caps have built up, but caps from previous pulses can still be seen. If fluid in the surface melt was flowing from the bottom of the structure to the top, the previous caps would be altered or destroyed. This observation suggests that the caps are formed through redeposition of material similar to VLS growth studied using nanosecond pulses.

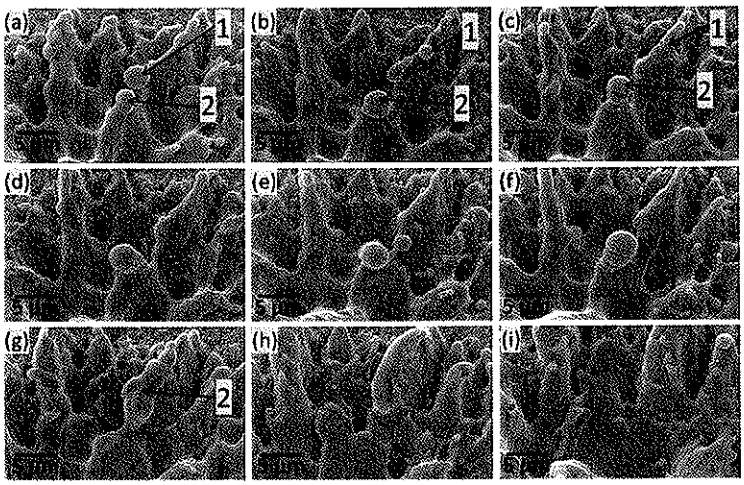

Fig. 7. (Multimedia online: Media 4 – 1.065 Mb, and Media 5 – 1.721 Mb; the videos are views of the same location at two different angles and at a lower magnification of the still image for a clearer view of the development) SEM image of stepped ASG-mound growth on nickel imaged at 45 degrees after (a) 55, (b) 56, (c) 57, (d) 58, (e) 59, (f) 60, (g) 65, (h) 70, and (i) 80 pulses. Marker 1 points to a sphere that elongates and combines with the side wall through fluid flow processes. Marker 2 points to an ASG-mound that grows taller with the formation of hemispherical caps formed through redeposition and then melts and combines with the sidewall at higher pulse counts.

The relative dominance of ablation pits during the third phase of development is an additional indication of a difference in dominant growth mechanisms between BSG-mounds and ASG-mounds. This major difference in formation between the late stages can be seen in Fig. 8 (multimedia online: Media 6). The top row is a series of images of BSG-mound formation during the third phase and the bottom row is of ASG-mound formation. Notice that with increasing pulse count, the BSG-mounds grow larger in diameter and some structures combine together to form even larger features. In some cases, the BSG-mounds overtake the pits (see pit marked 1). In the third stage of ASG-mound development, a different process begins to dominate. With increased pulse count pits continue to grow larger and combine together. Eventually the pits grow large enough that the ASG-mounds begin to disappear. This can be seen by the growth of the pits marked 2 and 3 in the bottom row of Fig. 8. With increased pulse count beyond what is shown here, the pits continue to grow larger until they

#185267 - $15.00 USD Received 13 Feb 2013; revised 22 Mar 2013; accepted 22 Mar 2013; published 29 Mar 2013

dominate the entire ablation crater. Eventually, the ablation crater will contain one large pit with no other microstructure.

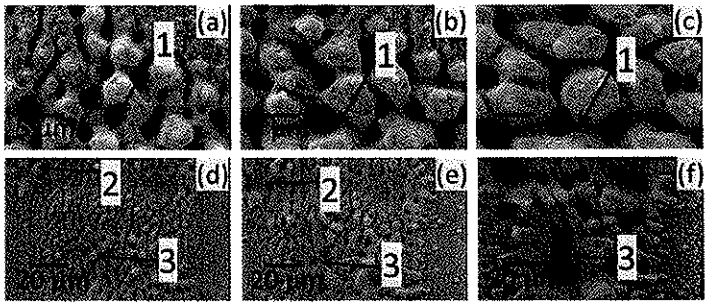

Fig. 8. (Multimedia online) Top row (Media 6 – 2.170 Mb): SEM images of stepped BSG-mound growth on nickel (200/201) after (a) 190, (b) 280, and (c) 500 pulses. Bottom row: SEM image of stepped ASG-mound growth on nickel after (a) 60, (b) 80, (c) 100 pulses. Marker 1 points to a pit that gets overtaken by BSG-mounds. Markers 2 and 3 point to ASG-mounds that get overtaken by pits.

Summary of growth mechanisms for BSG-mounds and ASG-mounds

A summary of the shot-by-shot development for two unique surface morphologies, BSG-mounds (F = 1.39 J/cm^2) and ASG-mounds (F = 3.08 J/cm^2), is shown in Table 1 and schematically in Fig. 9. This study indicates that the two morphologies form through different balances of PVA, fluid flow, and material redeposition. The balance of the dominant formation mechanisms is shown to depend critically on the laser fluence, which strongly determines the overall formation processes.

Table 1. Summary of shot by shot growth of BSG-mounds and ASG-mounds.

Phase 1: Formation of Precursor Sites	
BSG-mounds (~1-120 pulses)	**ASG-mounds (~1-30 pulses)**
Random nanostructure that increases in size and density with increasing pulses (~1-50 pulses)	Random nanostructure that increases in size and density with increasing pulses (~1-14 pulses)
Formation of microripples (~50-80 pulses)	Simultaneous formation of microripples, pits, and domes (~14-20 pulses)
Breakup of microripples into domes and pits (~80-120 pulses)	Formation of sharp peaks on ASG-mounds and increase in pit size (~20-30 pulses)
Phase 2: Development of multiscale structures	
BSG-mounds (~120-600 pulses)	**ASG-mounds (~30-150 pulses)**
PVA of surface to form BSG-mound structure (~120-140 pulses)	Combination of fluid flow and redeposition of ablated material causes ASG-mounds to grow above surface (~30-150 pulses)
PVA causes the height of BSG-mounds above the pit bottoms to grow taller (140-600 pulses)	Neighboring pits combine and continue to grow larger until they are the dominant surface feature (~30-150 pulses)
Phase 3: Final morphology	
BSG-mounds (~600 + pulses)	**ASG-mounds (~150 + pulses)**
Once formed, BSG-mounds and pits are ablated into surface at approximately the same rate (>600 pulses)	ASG-mounds stop upward growth as pits dominate (>150 pulses)
Increasing pulses cause the base of BSG-mounds to grow and merge with surrounding features (>600 pulses)	Eventually a single pit dominates and continues to ablate deeper into the surface (>150 pulses)

#185267 - $15.00 USD Received 13 Feb 2013; revised 22 Mar 2013; accepted 22 Mar 2013; published 29 Mar 2013

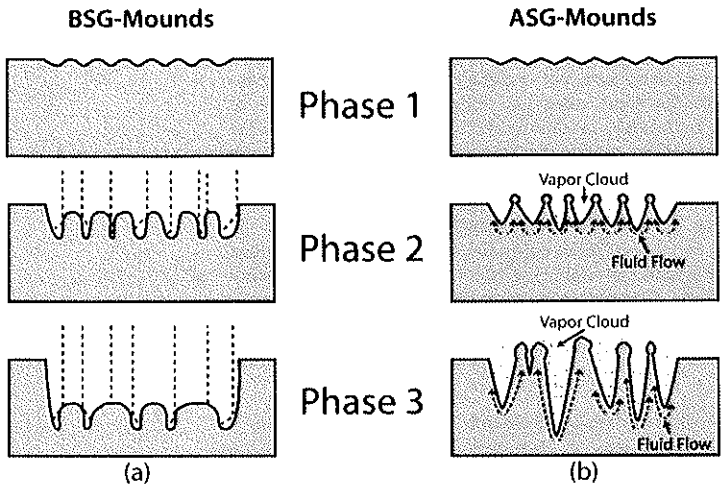

Fig. 9. Diagram of the formation of (a) BSG-mounds and (b) ASG-mounds through all three phases of development.

Most of the work on the formation of self-organized micro/nanostructures on metals using femtosecond laser pulses has focused on the formation of recessed structures similar to the BSG-mounds discussed here [14,15,34,39,40,45,48]. Some published work may contain images of structures similar to the ASG-mounds in this work, but there is no specific discussion on the difference in the structures and there is never a mention of the upward growth of the structures [13,32,37–39]. It should be noted that laser-induced periodic surface structures (LIPSS) lines are not associated with the formation of either BSG-mounds or ASG-mounds. In contrast, LIPSS with a period at or just below the wavelength of the incident light with an orientation perpendicular to the incident pulse polarization are present in many of the published works for microstructure formation on metals [13,34,37]. LIPSS have been studied on a number of materials [65] with the most complete theories presented by Sipe et al. [66,67] The reason that LIPSS are not observed here is due to the use of a flat-top beam profile as well as keeping the target substrate stationary with respect to the beam profile in this experiment as opposed to other published accounts in which beam profile was Gaussian and the sample was moved through focal region. LIPSS form at a lower fluence than the morphologies discussed here and are often observed on the outer rim of an ablation crater when using a Gaussian beam profile. Thus, the presence of LIPSS overlaid on top of the microstructures in other studies is likely due to the variation in fluence across the surface while rastering Gaussian pulses.

Conclusion

This paper presents for the first time detailed studies on the formation processes of two unique self-organized micro/nanostructure morphologies resulting from femtosecond interactions with nickel: ASG-mounds and BSG-mounds. The formation of such structures is broadly characterized by three phases: the formation of initial precursor sites via hydrodynamical processes, the development of multi-scale structures, and the evolution of the structures upon illumination with subsequent pulses. The laser fluence is shown to critically influence both the dominant formation mechanism and the resultant surface morphology, which results from a balance between PVA, fluid flow, and nanoparticle/material redeposition. The upward growth of ASG-mounds is due to a combination of fluid flow and

#185267 - $15.00 USD Received 13 Feb 2013; revised 22 Mar 2013; accepted 22 Mar 2013; published 29 Mar 2013

material redeposition, while the domination of the deep pits is from runaway PVA. With BSG-mounds, any fluid flow and redeposition that is present is overcome by ablation. PVA leads to the initial development of the microstructure, but eventually levels off and the peaks and valleys ablate into the surface at the same rate. The formation of these types of microstructures is often accompanied by LIPSS. In this work, LIPSS are not part of the formation mechanism and are not present at any step of the formation process. The formation mechanisms presented here are not only different for ASG- and BSG- mounds, but they are also different than previously described for silicon. There is a wide range of possible self-organized micro/nanostructures that can develop via femtosecond laser processing and the formation processes between them can be very different depending on the specific irradiation conditions and the properties of the substrate material. This study clarifies the shot-by-shot formation physics and growth mechanisms of femtosecond laser generated surface structures for two unique surface structure types, which is a significant step towards a broader understanding of the formation of multi-scale surface structures in a wide variety of materials.

Acknowledgments

This work has been supported by a Multi-University Research Initiative (MURI) No. – W911NF-06-1-0446, Grant Assistance in Areas of National Need (GAANN) No. – P200A070344, and a grant through the Nebraska Center for Energy Sciences Research (NCESR) with funds provided by Nebraska Public Power District (NPPD) to the University of Nebraska-Lincoln (UNL) No. 4200000844.

#185267 - $15.00 USD Received 13 Feb 2013; revised 22 Mar 2013; accepted 22 Mar 2013; published 29 Mar 2013